



**HAL**  
open science

## Development of a spatial risk assessment tool for the transportation of hydrocarbons: Methodology and implementation in a geographical information system

Florian Tena-Chollet, J. Tixier, G. Dusserre, J.-F. Mangin

### ► To cite this version:

Florian Tena-Chollet, J. Tixier, G. Dusserre, J.-F. Mangin. Development of a spatial risk assessment tool for the transportation of hydrocarbons: Methodology and implementation in a geographical information system. *Environmental Modelling and Software*, 2013, 46, pp.61 - 74. 10.1016/j.envsoft.2013.02.010 . hal-01799362

**HAL Id: hal-01799362**

**<https://hal.science/hal-01799362>**

Submitted on 24 May 2018

**HAL** is a multi-disciplinary open access archive for the deposit and dissemination of scientific research documents, whether they are published or not. The documents may come from teaching and research institutions in France or abroad, or from public or private research centers.

L'archive ouverte pluridisciplinaire **HAL**, est destinée au dépôt et à la diffusion de documents scientifiques de niveau recherche, publiés ou non, émanant des établissements d'enseignement et de recherche français ou étrangers, des laboratoires publics ou privés.

# **Development of a spatial risk assessment tool for the transportation of hydrocarbons: methodology and implementation in a Geographical Information System.**

F. Tena-Chollet, J. Tixier & G. Dusserre.

*Ecole des Mines d'Alès, LGEI, 6 Avenue de Clavières, 30319 Alès Cedex, France.*

*Florian.Tena-Chollet@mines-ales.fr*

J-F. Mangin.

*METL, DREIF/Service Sécurité Défense, Pôle préparation à la gestion de crise, 21-23, Rue Miollis, 75015 Paris, France.*

*Jean-Francois.Mangin@developpement-durable.gouv.fr*

## **ABSTRACT**

The transportation of dangerous goods is a complex issue involving various potential consequences for a wide range of high-stake elements. Most particularly, hydrocarbon transportation requires the carrying out of a global study in order to assess the risks involved. The aim of this study is to develop a prediction code for analyzing different possible hydrocarbon supply routes in order to determine whether modifying the flow of hydrocarbon transportation significantly increases the risk (for people, infrastructure and the environment). On the one hand, this paper details the methodology proposed for assessing risk levels using hazard scenarios and the vulnerability of high-stake elements. On the other hand, it presents the modeling tool developed (CARTENJEUX), based on an existing geographical information system (MapInfo), through a case study (Paris, France). Several maps (severity of accident, vulnerability and risk levels) generated using CARTENJEUX are presented in order to illustrate how stakeholders can determine preferential routes at regional scale.

**KEYWORDS:** GIS, risk assessment, dangerous goods transportation, decision making.

## 1 INTRODUCTION

In the event of a Dangerous Goods Transportation (DGT) accident, the nature and quantity of the products transported can generate various physicochemical effects (thermal flux, overpressure, toxic, radiological and corrosive effects, etc.). Another major cause of complexity is the multiplicity of circulation routes (highways, national, local, etc.), and the multiple causes of accidents (technical, organizational, human, natural). These factors make it difficult to define specific emergency plans, hence the necessity of proposing predictive methods to assess the risk level of these transportation activities.

Although the number of road accidents involving DGT is very low - 1.5% of total truck accidents (BARPI, 2005) - they can have a significant impact on the population and environment, especially regarding health, ecological, psychological and economic factors.

The main hazards associated with DGT accidents, which are similar to accidents involving fixed facilities, include the following dangerous phenomena: explosions, fires, emission of toxic or radioactive clouds, and atmosphere, water or soil pollution (BARPI, 2005).

Indeed, the hazard level of DGT can be catastrophic, and can occur at multiple points over a given territory. According to the French Ministry of Environment (DDT, 2007), among the 58 identified industrial accidents that have caused over 50 deaths since 1900, 23 of them concerned DGT. And among the most lethal, we can note: the crash of a propylene tanker at Los Alfaques (Spain) in 1978, which resulted in 216 deaths and dozens of injuries, and the pipeline leak at Ufa (USSR) in 1989, which caused 192 deaths and 706 injuries (BARPI, 2005).

Although there were no deaths, the Mississauga train derailment (Toronto) in Canada (10-16 November 1979) is of great interest, because it required the long-term evacuation of about 240,000 people, with several accidental phenomena, such as the BLEVE of a propane wagon and the toxic dispersion of chlorine.

In this context, the French authorities carried out a global study of DGT, more specifically hydrocarbon transportation and its associated risks, in the Ile de France region (including Paris). The objective was to determine whether increasing the flow of hydrocarbon transportation in Ile de France significantly increased the risk.

To respond to this question, it is necessary to assess both the DGT accident risk level and the vulnerability of high-stake sites. To reach this goal, a methodology of risk level assessment over a given territory was developed, based on the severity of the accident and the vulnerability of the area located close to the accidental phenomena in terms of the stakes involved (Dandrieux et al., 2006). This approach provides a risk level assessment for each point in the studied area so as to choose an optimized route for DGT. In order to optimize a set of routes (that is to say one or several roads) between two locations, risk maps can be produced. Furthermore, this spatial approach was implemented on the geographical information system (GIS) MapInfo, and a specific tool, named CARTENJEUX, was developed for stakeholders.

## 2 MATERIAL AND METHODS

### 2.1 *Examples of DGT risk analysis*

DGT is a very important topic in European countries and several researchers have proposed different approaches. General studies of DGT accidents have been carried out, for example Oggero et al. (2006), a survey of accidents involving the transportation of hazardous goods by road and rail. They identify the causes, consequences, material involved, severity and frequency of each one. They provide generic scenarios (event tree), generic causes of accident and accumulated probabilities of road/rail accidents based on the MHIDAS database in order to obtain an overview of DGT accidents.

Some risk analyses have also been developed at local level. These local studies are generally based on thorough analysis of the hazard, either using a probabilistic approach

to quantify an accident rate in function of road features (tunnel, bridge, highway, etc.) (Fabiano et al., 2002), or by means of F/N curves (Milazzo et al., 2010) and accident impact areas (Bubbico et al., 2004). Stakes are generally taken into account by the average population density near the road or the area of interest, in function of accident impact area (Bubbico et al., 2004; Bubbico et al., 2006). In the same way, Milazzo used population density and vulnerable elements (shopping centers, hospitals, schools, etc.) to describe the spatial distribution of human stakes (Milazzo et al., 2002). All these methods are generally implemented in a geographical information system to produce risk maps.

Concerning the assessment of the stakes attached to vulnerable elements located in the territory concerned, we can note that generally only human stakes are considered, in the form of average population densities [Verma, 2011]. A major limit is the fact that few approaches take natural and infrastructural stakes into account.

A classical approach was used to model the system and to qualify the question of risk assessment (Tixier et al., 2002). It is based on following the three elements: the source of the hazard, the hazard propagation flux, and the potential targets.

## 2.2 *Characterization of the study area*

The city of Paris covers an area of 2,723 km<sup>2</sup>, much smaller than the urban area of which it is the core. Suburban development has accelerated in recent years with an estimated total of 11.4 million inhabitants in 2005.

Paris' closest ring includes three adjoining districts which are fully saturated with urban growth. The ring of the four outside districts is only covered in their inner areas by Paris' urbanization. These eight districts form the larger administrative region "Ile-de-France", which includes a large number of high-stake economic, historical, touristic, cultural and natural sites.

Paris is located in the north-bending arc of the river Seine (Figure 1), includes two islands which form the oldest part of the city, and is bordered by two outlying parks (“Bois de Boulogne” and “Bois de Vincennes”).

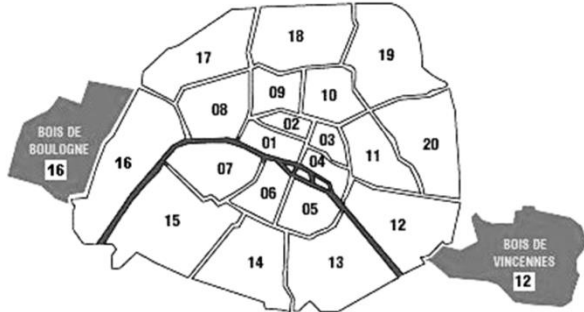


Figure 1: map of Paris.

Finally, because it is a capital and also the largest French city, Paris features many important and heterogeneous high-stake sites, whose sensitivity must therefore be considered in the risk studies.

## 2.3 *The proposed modeling procedure*

### 2.3.1 *Generalities*

In order to assess the risk, it is necessary to describe the studied system, which consists of three main elements (Figure 2): the source of hazard (a hydrocarbon tanker), the propagation of the effects in the environment (here only thermal radiation effects were considered), and the high-stake elements (classified in a typology).

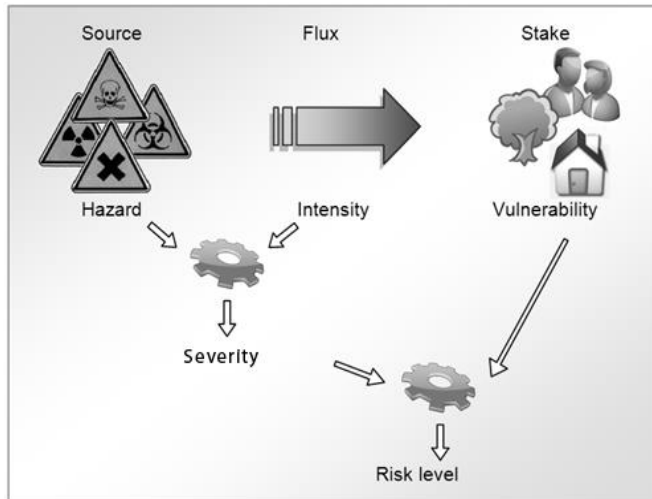


Figure 2: schematization of the studied system.

The risk level thus results from the contribution of two indexes:

- The accident severity, which takes into account the intensity of consequences, the accident frequency of a DGT and the rate of road accidents;
- The vulnerability of the high-stake elements along the hydrocarbon supply routes (Tixier et al. 2003).

So, the definition of the risk level (RL) is:

$$RL = f(Severity, Vulnerability)$$

In order to calculate these two main indexes, which are necessary to assess the risk level of a territory, spatial discretization must be performed. This principle can be applied using a geographic mesh composed of a set of cells (Figure 3) which have a specific size determined in function of the precision of the data used and the impact areas of accidental phenomena. For each cell, each index can be calculated in order: the severity, then the vulnerability, and finally the risk level. The first two indexes are normalized using a specific scale in order to assess the risk.

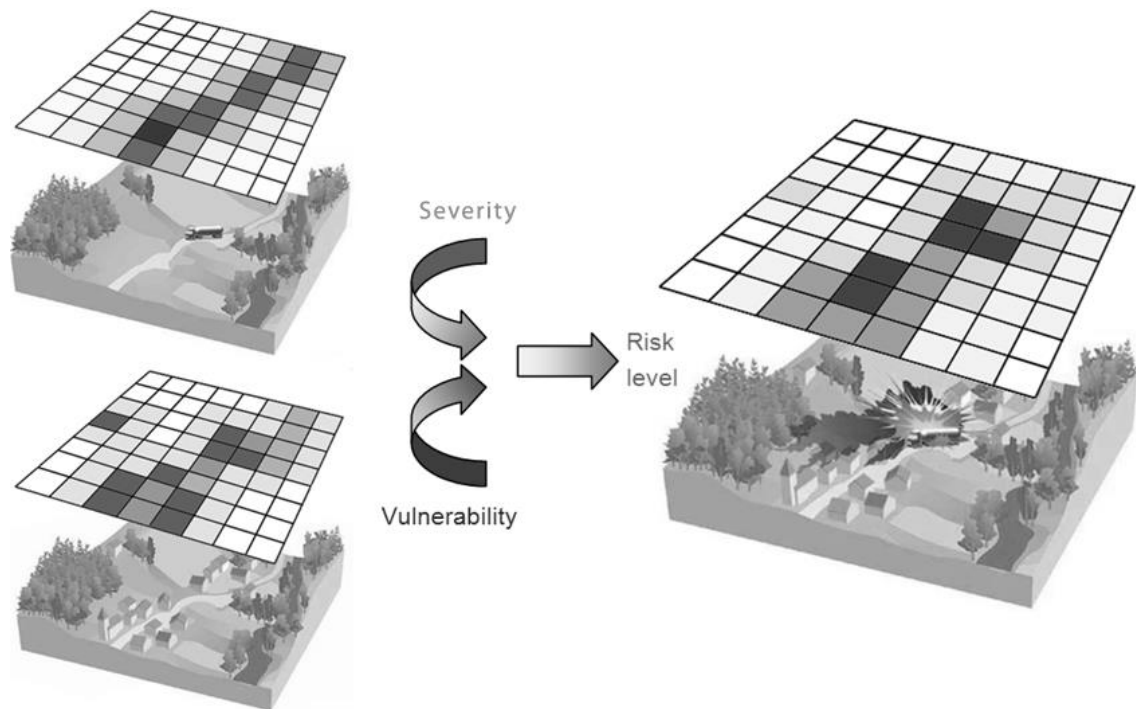


Figure 3: General approach to assess the risk level

The main advantage of this approach is that it provides visual mapping of the results and helps to understand the elements (severity and vulnerability) which contribute to the risk level.

### 2.3.2 Assessment of accident severity

The aim of the severity index is to include two dimensions: one deterministic, the other probabilistic. It is therefore described by means of two variables:

- The intensity of consequences of a DGT accident;
- The accident frequency on a specific route.

Hence, the severity index is defined as:

$$\textit{Severity index} = f(\textit{intensity of consequences, accident frequency})$$

The following parts explain the way to assess the intensity of consequences and accident frequency indexes.



### 2.3.2.1 Intensity of consequences

The intensity of consequences index (IC) takes into account the deterministic dimensions and the characteristics of accident scenarios. The IC of an accident is evaluated by the definition of effect areas which are based on specific thresholds defined in function of the type of high-stake element.

In order to define these effect areas, two sets of thresholds are used (MEDD, 2005): one for human stakes and another one for environmental and infrastructural stakes. It is important to call to bear in mind that DGT fire accidents involving hydrocarbons will impact the territory over no more than some hundreds of meters in most cases.

The first set for human stakes contains the following thresholds (Figure 4):

- 3kW/m<sup>2</sup>, irreversible effect threshold for the definition of the area of significant hazard to life;
- 5kW/m<sup>2</sup>, lethal effect threshold for the definition of the area of great hazard to life;
- 8kW/m<sup>2</sup>, significant lethal effect threshold for the definition of the area of very great hazard to life.

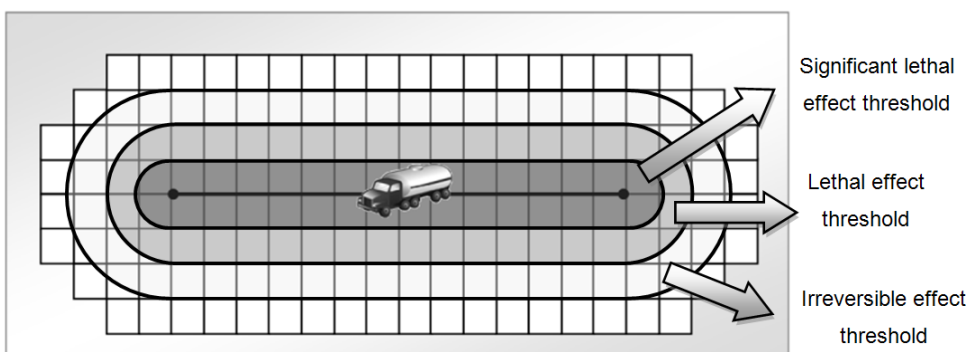


Figure 4: Intensity of consequences of a DGT on a road section.

The second set for environmental and infrastructural stakes consists of the following thresholds:

- 5kW/m<sup>2</sup>: threshold of significant broken windows;
- 8kW/m<sup>2</sup>: threshold of serious damage to infrastructures;
- 16kW/m<sup>2</sup>: threshold of very serious damage to infrastructures, apart from concrete;
- 20kW/m<sup>2</sup>: threshold of serious damage to concrete infrastructure;
- 200kW/m<sup>2</sup>: threshold of catastrophic damage to concrete for at least 10 minutes.

For each of these areas, an index value between 0 and 5 is assumed, as summarized in the following table:

<b>Thermal radiation thresholds</b>	<b>Severity index for human stakes</b>	<b>Severity index for environmental and infrastructural stakes</b>
3 kW/m <sup>2</sup>	1	NA
5 kW/m <sup>2</sup>	3	1
8 kW/m <sup>2</sup>	5	2
16 kW/m <sup>2</sup>	NA	3
20 kW/m <sup>2</sup>	NA	4
200 kW/m <sup>2</sup>	NA	5

Beyond the distances obtained for human stakes with a threshold of 3kW/m<sup>2</sup> and for environmental and infrastructural stakes of 5kW/m<sup>2</sup>, the value of severity is null (NA) by assumption.

In order to finalize the severity index, it is necessary to incorporate the accident frequency dimension.

#### 2.3.2.2 Accident frequency

The accident frequency index is based on the flow rate of DGT per year (Flux\_DGT), the length of the road (L in km) and the accident rate (RA in % per km).

The accident frequency index (that is to say the number of DGT accidents per year), for one section of road, is calculated as:

$$\text{Accident frequency} = L * RA * Flux\_DGT$$

Range of accident frequency	Index of accident frequency
$10^{-8} > \text{accident frequency}$	1
$10^{-7} < \text{accident frequency} < 10^{-8}$	2
$10^{-6} < \text{accident frequency} < 10^{-7}$	3
$10^{-5} < \text{accident frequency} < 10^{-6}$	4
$\text{accident frequency} > 10^{-5}$	5

### 2.3.2.3 Assessment of the severity index of a route

In order to obtain the value of the severity index of one mesh, it is necessary to take into account all the contributions provided by each road. So, the severity index of one mesh is calculated by the sum of each contribution from each road, knowing that a road is defined by its length, its rate of accidents and finally its DGT flow.

$$\text{Severity index}_{mesh} = \sum_{(1 \text{ to } n)} \text{Consequence intensity}_i * \text{accident frequency}_i$$

with  $i$  representing the number of roads influencing the mesh. In another words, the mesh undergoes the influence of  $n$  roads in term of consequence intensity and accident frequency in function of areas of effect defined by thresholds.

### 2.3.3 Assessment of the vulnerability of high-stake elements

#### 2.3.3.1 Research question

The aim of the vulnerability index is to assess the danger to high-stake elements if exposed to a potential hazard. To reach this goal, the critical or sensitive elements

within the territory must be identified, geolocated and weighted to assess their relative importance (Tixier et al. 2012). The idea developed is to identify and characterize the vulnerability of the elements located in the surroundings of a DGT route. The following figure summarizes the problem, which aims to answer the following question: is Area #1, which contains human, environmental and infrastructural high-stake elements, more or less vulnerable than Area #2, which also contains human, environmental and infrastructural high-stake elements, but different in quantity and nature?

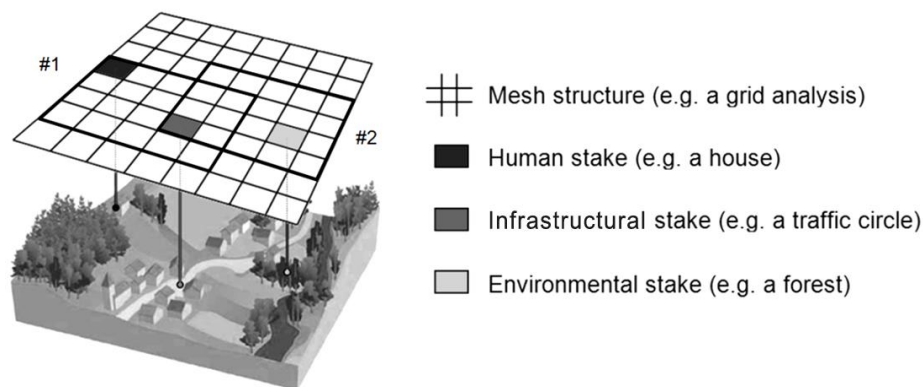


Figure 5: question of the definition of vulnerability.

To answer this question, it is necessary to characterize the study area (see “3.1. Data and Databases used”), then to define the stakes. A specific methodology for the assessment of the vulnerability, based on the work performed during the European project ARAMIS (Tixier, 2006), can be used. This methodology includes a semi-quantitative approach (a multicriteria decision method named the “Saaty Method”) which depends on expert judgments. The analytical hierarchical process (AHP) can be used for multicriteria assessment problems (Marinoni et al., 2011) in order to score global objectives in an easy way by including the judgments of stakeholders or other key people (Zerger et al., 2011). This provides a broad-based representative view of expert opinion concerning a studied domain (Chen et al., 2011). The main criticism of the AHP approach is due to the “rank reversal phenomenon” which can lead to a change in the ranking of two options when a new one is include (DCLG, 2009; Zerger et al., 2011). We must therefore ensure that the choice of options used to describe the risk ranking system is exhaustive.

### 2.3.3.2 Saaty multicriteria decision method

The purpose of the Saaty method is to assess priorities. To this end, the first point is to have a consensus regarding the objective, and secondly to break down the complex and unstructured situation into its main components. The types of results can be a classification, the allocation of numerical values regarding subjective judgments, or the aggregation of judgments to determine the criteria with the highest priorities. The multicriteria hierarchical method enables decision-making by a group in a consensual way due to a better coherence of judgments, through the construction of a linear additive model (Chen et al. 2011).

Saaty's multicriteria hierarchical method (Saaty, 1984) is based on four main steps:

- A description of the studied system (some elements and criteria are proposed in order to characterize the situation);
- The construction of hierarchies (to organize the elements and the criteria to respond to the question);
- An assessment of priorities (based on expert judgments);
- Validation of coherence.

The construction of a hierarchical structure requires the creation or identification of links between the various levels of that structure.

Each element or criteria of a hierarchical structure is situated at a given level of the structure. The upper level corresponds to the global objective (or dominant element). The elements of a given level are ranked by binary comparison according to their impact on an element at the next highest level, in order to the elements. The various levels of a hierarchy are, consequently, interconnected.

A complex situation can be analyzed by a systematic approach with the help of such a hierarchical structure. The priorities have to be assessed. This process is performed by comparing elements two-by-two (binary comparison). This ranks the elements according to their relative importance. Finally, the logical coherence of the structure is

validated to confirm the whole applied process. To make the binary comparisons, it is necessary to use a scale based on standard numerical variables or more qualitative variables that help to take into account qualitative aspects.

From this definition and from hierarchical structures, the matrices and functions of the vulnerability index are deduced. The matrices are translated into a questionnaire which enables experts' judgments to be gathered for the evaluation of each coefficient of the vulnerability functions.

A simple example of the application of the Saaty method is presented below. If we define the vulnerability as a function of criteria A, B and C and of elements w, x, y and z, the following hierarchical structure (Figure 6) can be built.

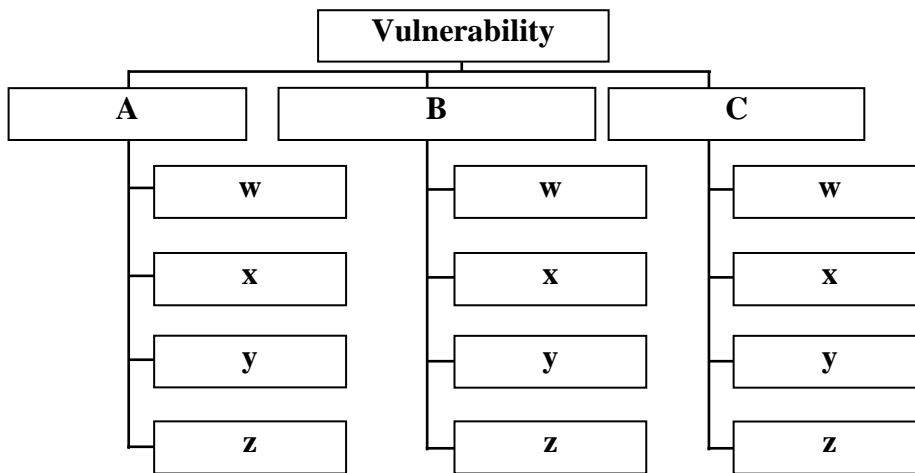


Figure 6: example of hierarchical structure.

If we consider the top of the hierarchical structure in Figure 6, the following matrix is deduced in order to make binary comparisons (and to define the priorities):

V	A	B	C
A	1	X1	X2
B		1	X3
C			1

where X1, X2 and X3 are the weighting factors provided by experts through a questionnaire. The questionnaires are analyzed by inverse methods to retrieve the weighting factors. From this matrix, eigenvectors can be calculated and named  $\alpha$ ,  $\beta$  and  $\gamma$ . In another words, each of these values gives the relative importance of each criterion. The vulnerability (V) is thus a function of the vulnerability criteria A, B and C.

$$V = \alpha \times A + \beta \times B + \gamma \times C$$

With  $\alpha$ ,  $\beta$  and  $\gamma$ , the vulnerability factors of the vulnerability function.

A specific processing operation was required to aggregate the experts' judgments. Each judgment was aggregated by the use of the geometrical mean. A single questionnaire was thus obtained, which was an aggregation of the judgments of all the experts consulted. All the judgments are added to the matrices and the vulnerability factors assessed as presented below.

In order to validate the vulnerability factors, the Consistency Ratio (CR) is assessed and must be less than 10%.

$$CR = (CI) / (RI).$$

Where

**CI** is the Consistency Index, with  $CI = (\lambda_{max} - n) / (n-1)$  and  $n$  the number of compared elements.

$\lambda_{max}$ . is the maximum eigenvalue (Perron root) of the matrix.

**RI** = Random Index. For each matrix of size  $n$ , Saaty's team generated random matrices and computed their mean **CI** value and called it the Random Index.

### 2.3.3.3 Study area and high-stake element typologies

The aim of this section is to define the territory subject to DGT hazard in order to determine the risk level. It is therefore necessary to propose a set of types of high-stake element so as to accurately characterize the environment. It is necessary to find the right

balance between the number of site-types to be taken into account and the limitations due to the multicriteria decision method.

First of all, sites were divided into three categories in function of the stakes involved, and each of them detailed in a list of generic types of high-stake element:

- Human (H)
  - o Private dwelling (H1)
  - o People present in a public assembly building (H2)
  - o Users of communication networks (H3)
- Environmental (E)
  - o Agricultural area (E1)
  - o Natural area (E2)
  - o Specific natural area (E3)
  - o Wetland or water body (E4)
- Infrastructural (I)
  - o Industrial site (I1)
  - o Public utility or infrastructure (I2)
  - o Private structure (I3)
  - o Public structure (I4)

As described above, Saaty's multicriteria hierarchical method (Saaty, 1984) is based on three main steps, once a system has been described:

- construction of hierarchies;
- assessment of priorities;
- validation of coherence.

The construction of a hierarchical structure requires the creation or the identification of links between the various levels of this structure. In order to have a good understanding of the situation, the description of the environment is completed by a typology of impacts due to exposure to thermal radiation. Three impacts due to thermal radiation are considered to characterize the effects of major accidents on high-stake element:



- Integrity impact, which respectively qualifies the human, environmental and infrastructural damage;
- Economic impact which qualifies an effect in terms of loss of production or of rehabilitation;
- Psychological impact which qualifies an effect in terms of influence on a group of people.

It is then necessary to organize these typologies in order to respond to the vulnerability question. The next step therefore consists in structuring the information in accordance with the following definition of the vulnerability: the vulnerability of each type of high-stake element in function of thermal radiation effect is evaluated by binary comparison using the three impact types as characterization criteria.

The result is the vulnerability of one class of high-stake element to a thermal radiation effect. The associated hierarchical structure for human vulnerability is presented in Figure 7. In this hierarchical structuration, each category of human element is compared in function of each criterion (integrity, economic and psychological impact).

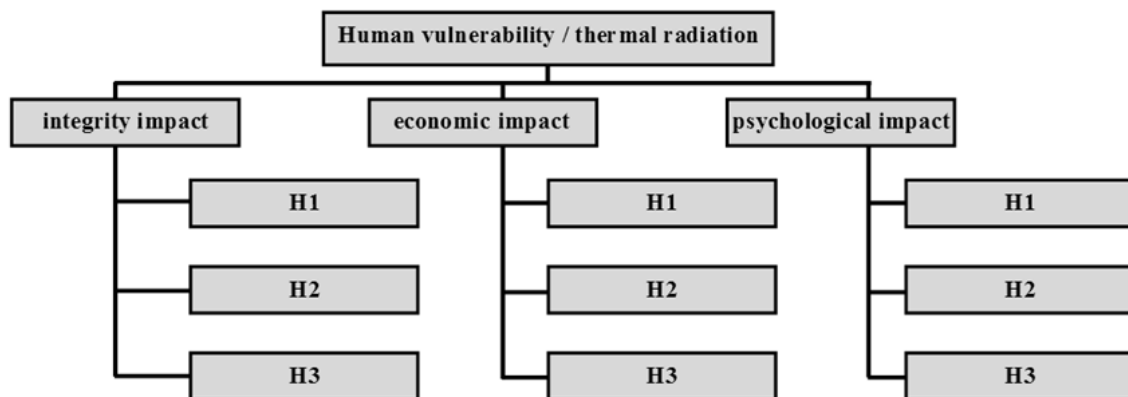


Figure 7: hierarchical structure for human vulnerability.

The same hierarchical structure applies to environmental and infrastructural vulnerability. The matrices and functions of the vulnerability index are deduced from this definition and the hierarchical structures. The matrices are translated into a questionnaire which helps to collect the expert judgments for the evaluation of each vulnerability coefficient of the vulnerability functions.

Thirty eight experts had already been individually consulted during the ARAMIS European project (Tixier et al., 2006). The breakdown of experts by type is presented in Figure 8: about 60 % were risks experts (from public or private organizations), while the remaining 40% were industrialists or local authority employees.

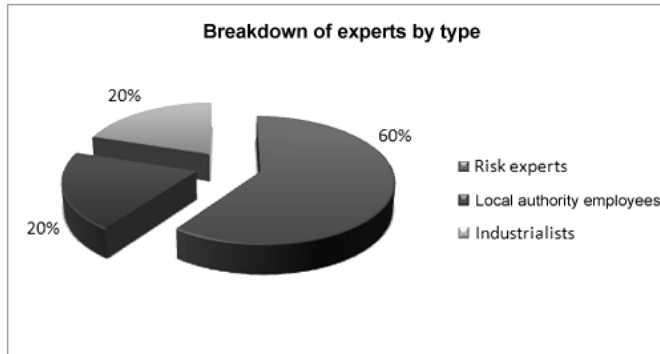


Figure 8: Breakdown of experts by type.

A specific processing operation was performed to aggregate the judgments of the above-mentioned experts. Each judgment was aggregated by means of the geometrical average, producing a new questionnaire which is the aggregation of the judgments of all the experts consulted. All the assessments obtained were assessed into the matrices and the vulnerability factors could be assessed. The results are given in the next paragraph.

To assess the vulnerability factors of each function, the eigenvectors of the matrixes must be calculated. The results correspond to the factors of vulnerability and we can see that all the Consistency Ratios (CR) have a value lower than 10%. The following table presents the results for the human, environmental and infrastructural vulnerability functions.

<b>Human vulnerability – thermal radiation</b>	<b>CR %</b>
$VHft = 0,648 \times VHftS + 0,122 \times VHftE + 0,230 \times VHftP$	0.3
$VHftS = 0,548 \times H1 + 0,249 \times H2 + 0,203 \times H3$	1
$VHftE = 0,593 \times H1 + 0,268 \times H2 + 0,139 \times H3$	0.86
$VHftP = 0,400 \times H1 + 0,400 \times H2 + 0,200 \times H3$	0

<b>Environmental vulnerability – thermal radiation</b>	
$VEft = 0,550 \times VEftS + 0,240 \times VEftE + 0,210 \times VEftP$	1.58
$VEftS = 0,195 \times E1 + 0,231 \times E2 + 0,426 \times E3 + 0,148 \times E4$	2.54
$VEftE = 0,227 \times E1 + 0,227 \times E2 + 0,424 \times E3 + 0,122 \times E4$	0.57
$VEftP = 0,200 \times E1 + 0,200 \times E2 + 0,400 \times E3 + 0,200 \times E4$	0
<b>Infrastructural vulnerability – thermal radiation</b>	
$VIfT = 0,443 \times VIfTS + 0,387 \times VIfTE + 0,169 \times VIfTP$	1.58
$VIfTI = 0,246 \times I1 + 0,298 \times I2 + 0,21 \times I3 + 0,246 \times I4$	3.36
$VIfTE = 0,400 \times I1 + 0,200 \times I2 + 0,200 \times I3 + 0,200 \times I4$	0
$VIfTP = 0,142 \times I1 + 0,286 \times I2 + 0,286 \times I3 + 0,286 \times I4$	0

#### 2.3.3.4 Quantification factors

The quantification factors determine the level of stakes in the study area. A quantification factor is defined as a dimensionless variable, assuming values in the range 0-1, where 0 indicates the absence of the stake in the area and 1 indicates that the quantity of this stake in the area reaches its expected maximum.

## 2.4 *Development scheme*

### 2.4.1 *Global use cases*

In a preliminary study, the actors and interactions of the system were defined in order to construct the messages intended to be exchanged with the users. These specifications were further refined using various UML (Unified Modeling Language) models. As shown in Figure 9, the following four fundamental steps can be identified as being required:

- The manual selection of a road route (1): the user first selects a sequence of road segments which can be considered as a route for the hydrocarbon transportation;
- The generation of an analysis grid to cover the study area (3): square cells are created in order to divide the environment into a set of meshes. The spatial analysis can be made more or less precise by adjusting the size of each mesh;

- Cross-analysis (territory assessment) of the grid with other layers of the Geographic Information System (4): the properties of each object covered by a mesh are aggregated and associated to the mesh;

- Thematic analysis for viewing the results (6): this step displays the results from a human, infrastructural or environmental point of view, with an absolute or relative scale of view.

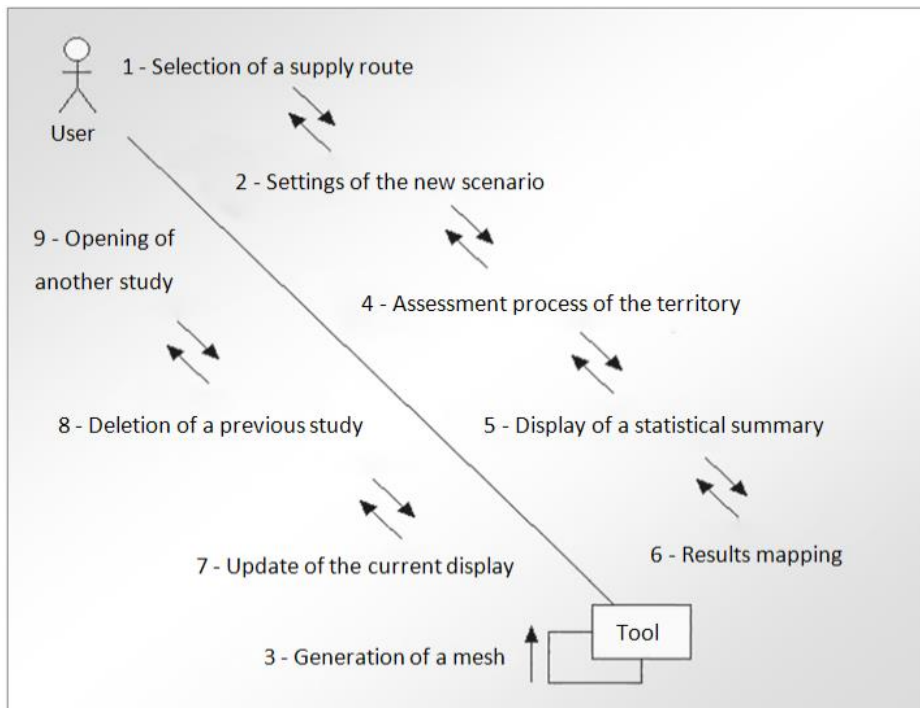


Figure 9: dynamic context diagram of the tool.

The tool uses a batch processing operation (Step 3, Figure 9) to schedule and automate a set of operations and computations which form its kernel. Several difficulties occurred during the software modeling and development: the main ones are detailed in the following section through some of the implemented algorithms.

## 2.4.2 Quick survey of the main algorithms implemented in the kernel

### 2.4.2.1 Grid creation process

The method selected for creating the grid is recursive construction of each cell, as shown in Figure 10. The size choice for the cells depends on the following two

constraints: the accuracy of the geography database and the distances of thermal radiation effects for the studied hazard scenarios (see Section 2.3.2). By assumption, we set up a size of 50 meters for the cells of each grid.

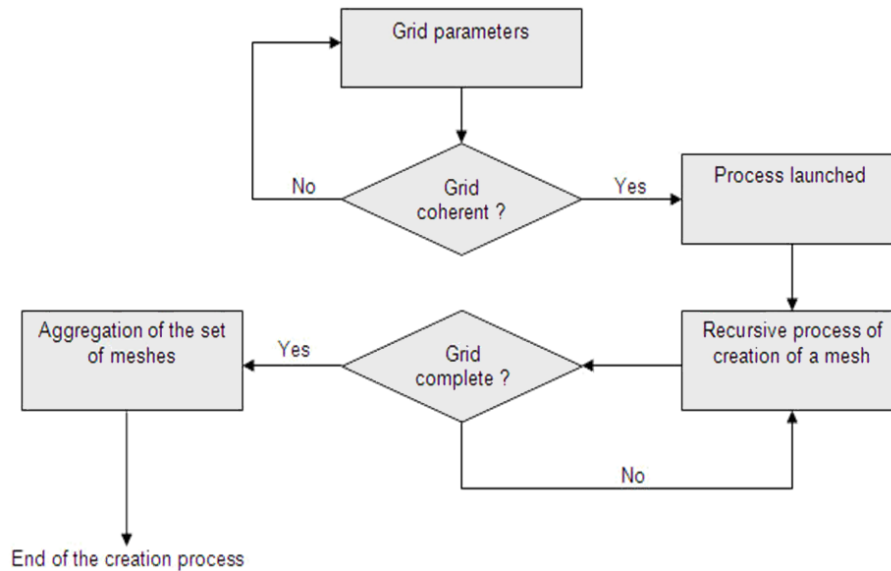


Figure 10: generation grid algorithm.

The primary focus is in fact to choose between the two main possible strategies in order to cover a territory with an analysis grid made up of square meshes.

The first one consists in the creation of a simple rectangular grid for all the studied territory (here, the city of Paris) thanks to a basic algorithm based on a variable which increments the rows/columns indexes to add each cell. This common approach can be implemented simply and quickly but the high number of meshes potentially created for an extended territory and which have to be crossed with GIS layers may cause significant time problems in the subsequent computational processes.

The second one only deals with the geographical areas of interest (here, the road sections plus the distances of thermal effects). It is thus possible to improve the processing time, but this approach requires a specific algorithm to cover only the targeted parts of the territory.

Therefore, it can be suggested to operate all road sections with the following sequential process: creation, georeferencing, union into a unified grid. In the existing data, each road section is a polyline object which can be composed of several linear segments. Each section of a given road is split into unitary segments which are covered by

intermediate sets of meshes. The created cells can be unified when all segments of all sections of all studied roads are processed. The following figure summarizes the mechanism as it was conceived during this design phase.

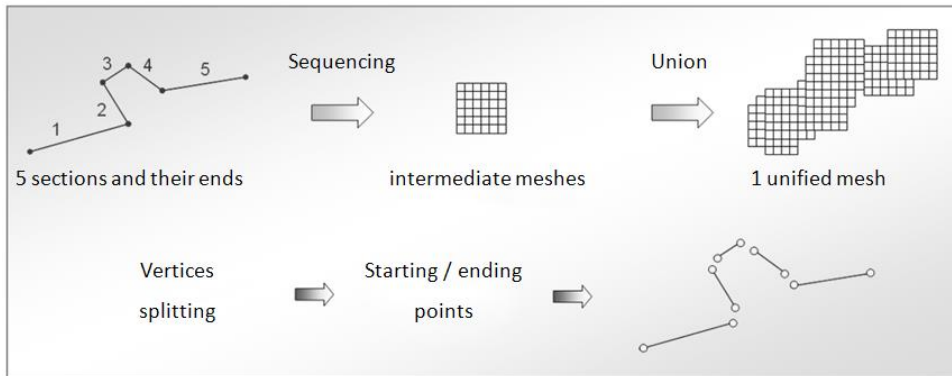


Figure 11: first algorithm tested.

#### 2.4.2.2 Coverage problem and clipping solution

However, a coverage problem occurred in the meshing of many routes due to their self-structure. In fact, these objects are defined as polylines in order to describe the road network. Figure 12 shows the benchmarks, i.e. the starting and the ending points, used in the meshing process of a road section,.

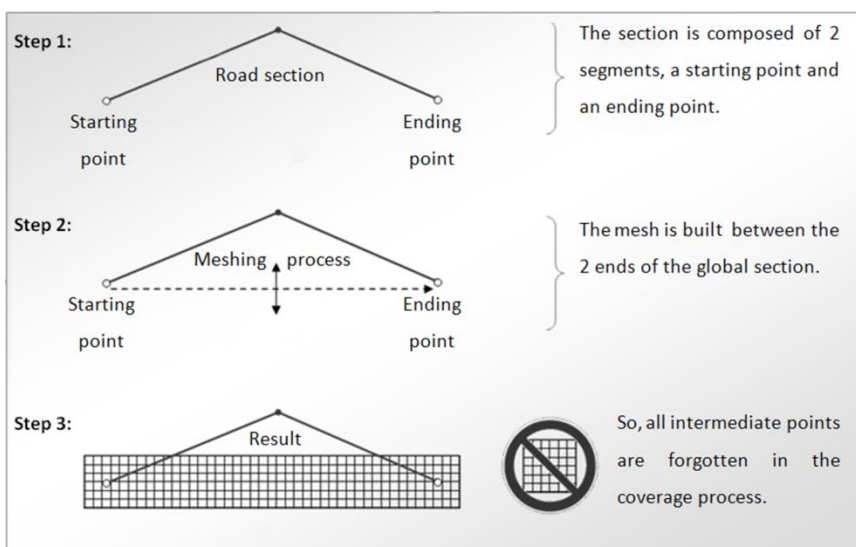


Figure 12: coverage problem of the first meshing algorithm.

This problem was solved by improving the first algorithm in order to browse (temporary clipping) each unitary segment (single line) of each road section (polyline). For the rest, the initial principle was retained (Figure 13).

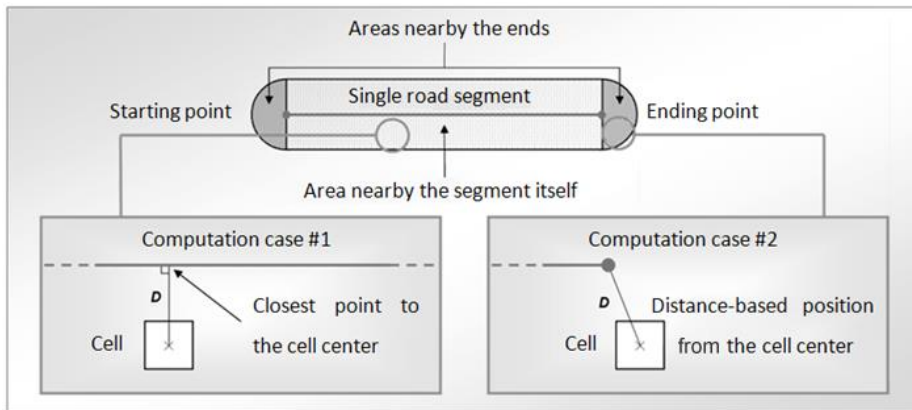


Figure 13: the two main mechanisms of the second meshing algorithm.

#### 2.4.2.3 Homogeneity problem and magnetic arrangement

Nevertheless, new unexpected results concerning the grids' homogeneity occurred. With the method employed, each mesh was generated by following the direction of its associated road segment, which meant that the cells were not drawn using the same reference points (Figure 14).

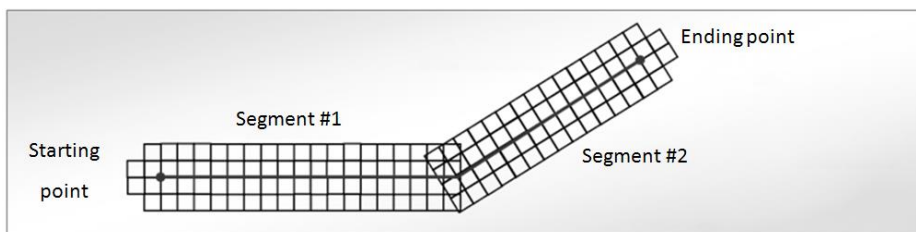


Figure 14: homogeneity problem of the second meshing algorithm.

In order to solve this problem, we created a specific method named “magnetic arrangement” in order to set all meshes in the same orthonormal basis. But this approach resulted in a final problem, as shown in Figure 15 below.

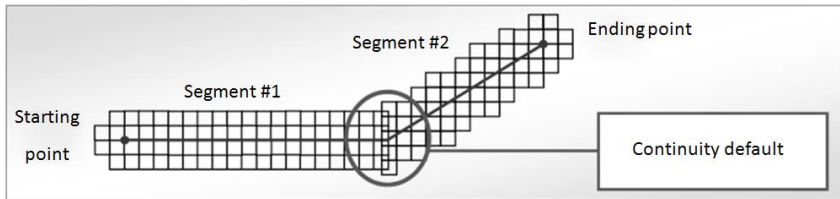


Figure 15: continuity problem between magnetized grids.

#### 2.4.2.4 Continuity problem and enhanced magnetic arrangement

To correct this lack of continuity, we had to set up a unified magnetic grid (we developed a method named “enhanced magnetic arrangement”) to calibrate each intermediate mesh with its neighbors in order to finally obtain a uniform continuous set of meshes. Figure 16 shows the mechanism used for the grid calibration.

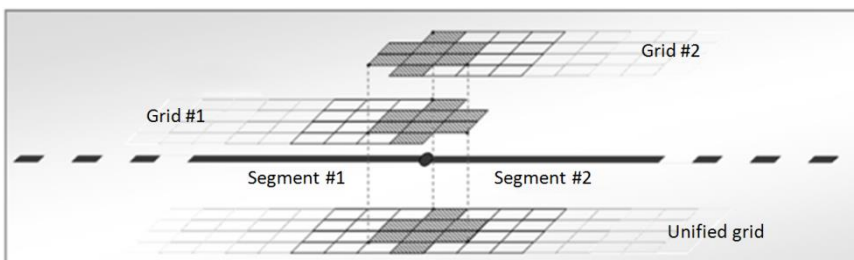


Figure 16: “enhanced magnetic arrangement” of two sets of meshes.

Figure 16 highlights furthermore the inevitable presence of repetitions (grayed cells): the ending point of a segment may also be the starting point of another one. These specific cells located at the ends of road segments can be removed by a method which we developed to verify the unicity of the individual elements making up the grid.

### 3 SOFTWARE

#### 3.1 *Data and Databases used*

The first step in the work consisted in describing the expected data. Its aim was to define which inputs will be used in the risk assessment model and the index calculation



processes for one or several routes selected by the user. The cartographic data required are:

- A description of the typology of the human, infrastructural, environmental high-stake elements present in the study area;
- A recent census of the population;
- A road network with traffic data specific to DGT, and accident rates.

Three cartographic database tables were used in order to describe the required data (Figure 17). The data used were calculated with average values over a year (2003). The structure and content of these tables are confidential, but it is important to say that the information precision is 20 meters.

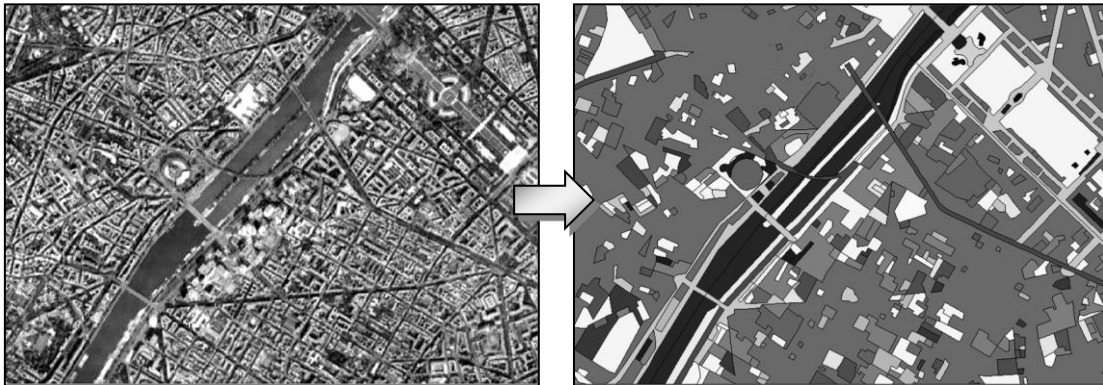


Figure 17: an orthophoto and its vectorial layer of population densities.

The main constraint relates to the type of existing map objects included in the database used: surface objects and polylines.

Indeed, the methodology takes as input the length of each route section: that is why it is necessary to manipulate line segments (polylines in a GIS) for the roads. But it is also essential to include each high-stake element (described by surface objects) prorated to their surface area in order to integrate territorial disparities into the meshing structure.

For this project, the French stakeholders provided very detailed databases of the territory of interest, but it is important to say that it may be difficult to obtain such quality for another region.

### 3.2 *General algorithm*

The main process implemented is based on four steps:

- The manual selection of a set of routes (one or more roads) by the user;
- The automatic generation of an analysis grid along this route;
- The cross-analysis between the grid and the GIS layers;
- The assessment of the risk for DGT.

The risk assessment step uses at the same time the high-stake element typology defined by the methodology and a grid. Figure 18 illustrates the cross-analysis operation between a grid and GIS layers in order to extract the expected data.

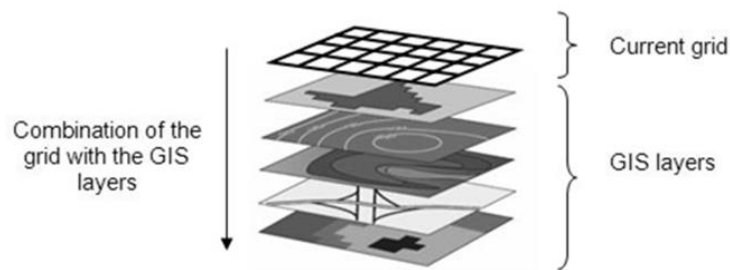


Figure 18: illustration of the cross-analysis between a set of meshes and GIS layers.

The process is designed like a transverse mechanism associating information about the human, infrastructural and environmental stakes into each mesh. All data are calculated taking into account the size and the area of meshes (densities of surface objects, proportional lengths of polylines). Subsequently, the results are stored in the GIS table which contains the analysis grid (MapInfo file format).

### 3.3 *GIS-based tool “CARTENJEUX”*

The final tool implemented to study hydrocarbon supply routes was based on a Geographical Information System. This software named CARTENJEUX, which means “stakes-based mapping” in French (figure 19), is in the form of an add-on (Ayrat, 2010) which aims to assess human, infrastructural and environmental risk.

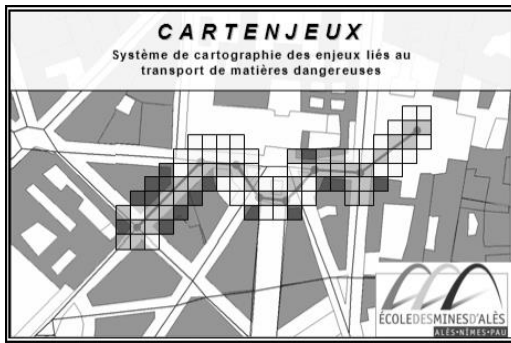


Figure 19: welcome page of the software.

### 3.4 *Route selection*

In order to study a route through grid analysis, it is necessary first to select linear objects directly on the GIS road layer. This solution has the advantage of being visual and concrete for the user since it physically indicates the road segments with which he/she wants to work. That is why the selection tools available in MapInfo are very useful because they offer a varied panel of possible selections of linear objects (for example, road sections).

### 3.5 *Grid generation*

Once a set of road segments has been made up, the user can configure a mesh size (in meters) for the grid building and a dimension (also in meters) on both sides of the axis, indicating the spreading of the grid around the road axis. This last distance is obtained in function of effects thresholds and can be entered by means of a specific user-friendly interface for the grid generation settings. Users hence have the capability of changing the size of the grid at run time.

It is important to say that the tool allows the user to manage a set of grids. Indeed, it is possible to display two routes currently loaded in memory in order to compare them. When several grids are shown simultaneously, the user can select one of them in order to choose the set of meshes on which the next operations will be done (statistics for example).

At this stage, the generation parameters are validated and the program starts the construction of the grid. As a result, the meshes created are aggregated in a unified grid, ready to be used to assess the risk of the covered territory.

### 3.6 *Cross-analysis of the grid with stakes layers*

A dynamic grid is now created and saved in a specific MapInfo table, whose fields are empty. This table has both upper and lower bounds, and all the cells of the grid are contiguous within those bounds.

So, the risk assessment process consists of cross-analysis, iterating all the cells objects in order to aggregate them with the data layers opened in MapInfo.

In the end, all the table's fields are assigned by quantification factors about each class of stakes.

### 3.7 *Risk assessment and thematic analysis*

At this stage, the functions of calculations specified in the methodology and implemented in the tool are launched in order to exploit the aggregated stakes data. Once the territory is evaluated, a module of thematic analysis assists the user to enable him or her to quickly visualize the severity index, the index of human, infrastructural and environmental vulnerability or risk level (Figure 20).

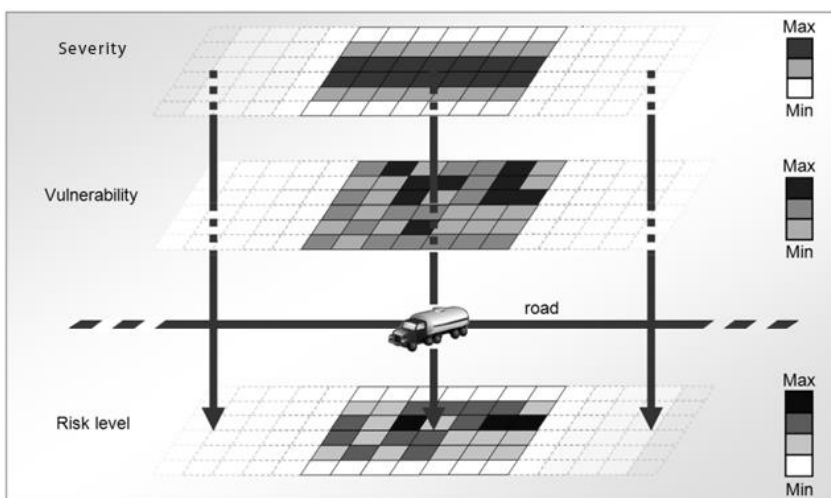


Figure 20: the three data layers mappable by CARTENJEUX.

In fact, this module is equivalent to a thematic map browser which proposes standard scales of visualizations (relative or absolute) in a few mouse-clicks. The user is thus able to obtain several maps about the severity of a potential accident, the vulnerability of high-stake elements, and the different levels of risk of the initial DGT route.

## 4 RESULTS AND DISCUSSION

It is important to say that the exact location of hydrocarbon tanks and the precise supply routes are sensitive and therefore confidential. The examples presented in the following sections are fictive, and any similarity to actual routes would be purely coincidental.

### 4.1 *Overview*

In order to illustrate the results given by the cartographic tool CARTENJEUX, this part shows an example (Figure 21) of two possible supply routes (named route 1 and route 2) between an hydrocarbon tank and a gas station (respectively named A and B). The objective is to compare the risk of the two routes from a human, environmental and infrastructural point of view, thanks to spatial and statistical results. This first example is just theoretical because the real supply routes chosen by French stakeholders are confidential.

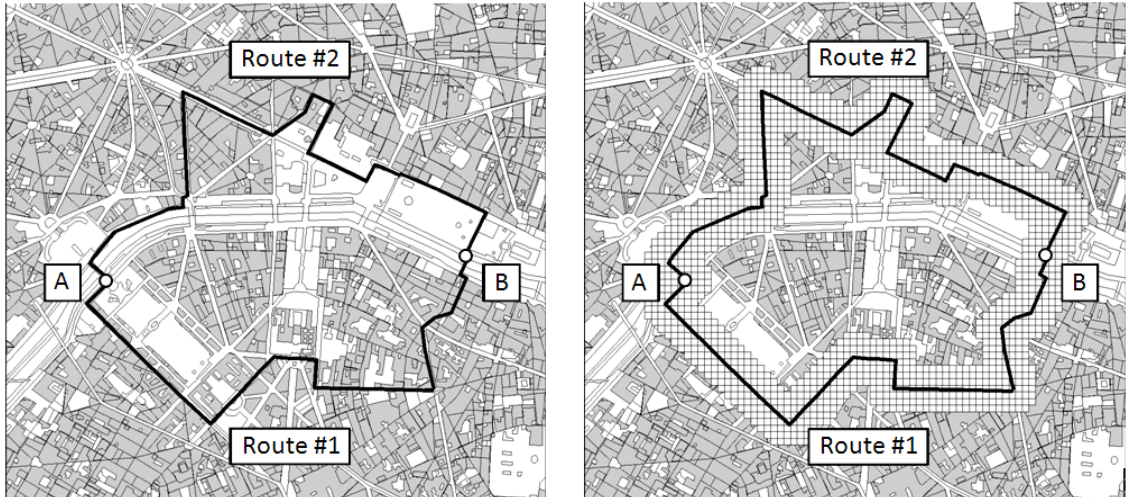


Figure 21: two possible routes between A and B (left) with their analysis grids (right).

Two grids are automatically created by the developed routines around each road axis. The different assessments will be run later, in order to obtain a map of risks. Figure 21 shows the two study areas before the cross-analysis.

In a last step, the analysis begins and displays the spatial results. Figure 22 indicates the human vulnerability in the surroundings of the two chosen routes. It is possible to see directly many disparities thanks to the use of cells which enable the consideration of one particular high-stake element group. A function is also available to specify the transparency of the grid in order to consult the subjacent layers and the thematic analysis simultaneously.

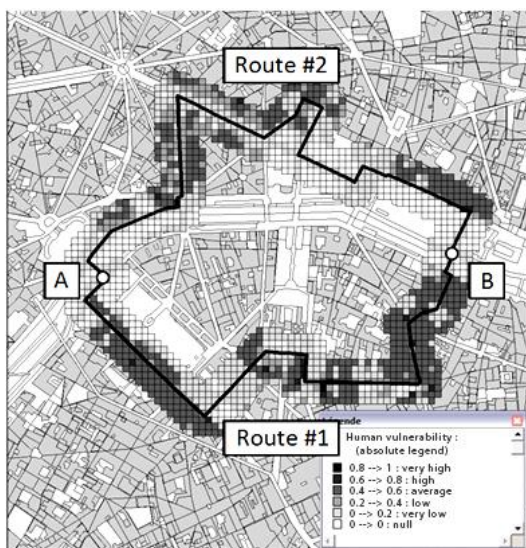


Figure 22: human vulnerability around two routes.

The dark gray cells indicate the presence of critical human high-stake elements which are due to highly urbanized areas.

In order to compare more precisely the two routes, the cartographic tool produces a statistical index of risk, as shown in the following figure. Indeed, the user can compare the evolution of the human, infrastructural and environmental risk levels (RL).

<b>Route #1</b>	<b>→</b>	<b>Route #2</b>
Human RL	↘ 23 %	Human RL
Environmental RL	↗ 65%	Environmental RL
Infrastructural RL	↘ 3 %	Infrastructural RL

Figure 23: evolution of the statistical index of risk between two supply routes.

In this example, the first route presents the lowest environmental risk level, whereas the second one leads to a decrease in the human and infrastructural risk levels. Thereby, this synthesis approach helps the user to understand the impacts of the two possible supply routes: in a highly urbanized area and if the environmental stakes are not overriding, the second route may be preferred.

In the previous figure, the main differences between the two routes were the human and environmental risks. The move from 1 to 2 would involve a reduction of 23% for the human stakes risk and a rise of 65% for the environmental ones. With regard to the infrastructural stakes, the analysis shows there is a light reduction in vulnerability of 3%.

#### 4.2 *Further details*

The accuracy of the cartographic data led to an analysis of a cell size in order to obtain a fair compromise for mitigating the error factor during the meshing process of the road

network. Accordingly to the geometric precision of the database (about 20 meters), a cell width of 50 meters was validated.

With the help of CARTENJEUX, different kind of maps can be obtained. The following examples (figures 24, 25, 26) concern several routes of supply for which the severity, the vulnerability and the global risk has been quantified. This analysis concerns all the territory of “Ile de France”, but only an extract of the results is presented for reasons of confidentiality.

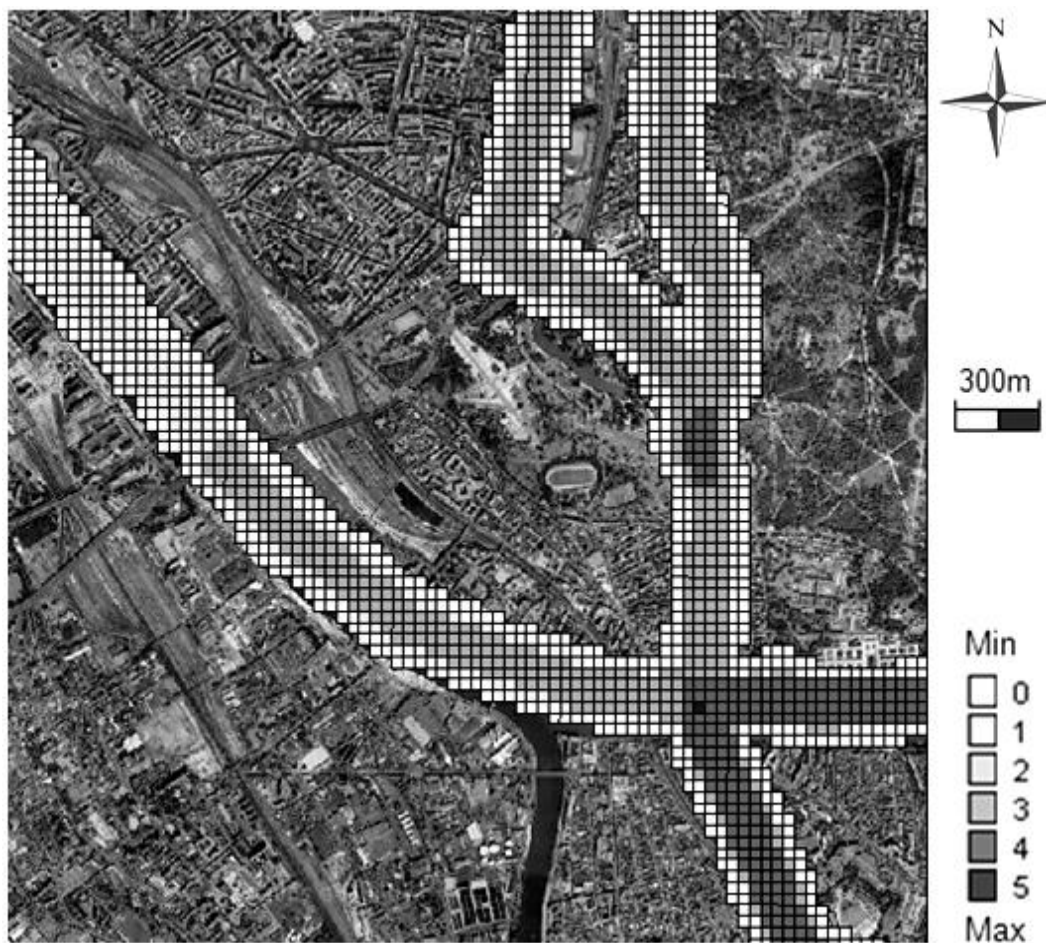


Figure 24: map of the severity index.



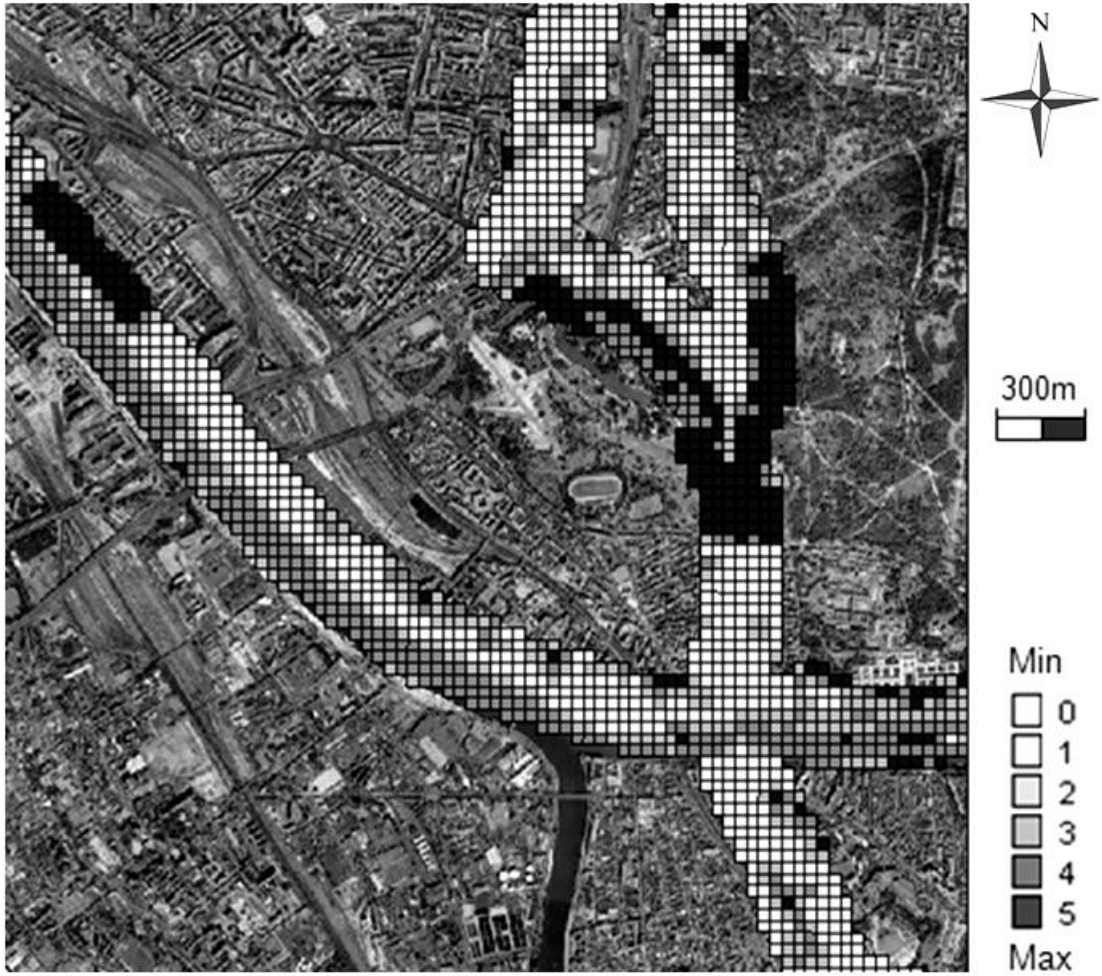


Figure 25: map of environmental vulnerability.

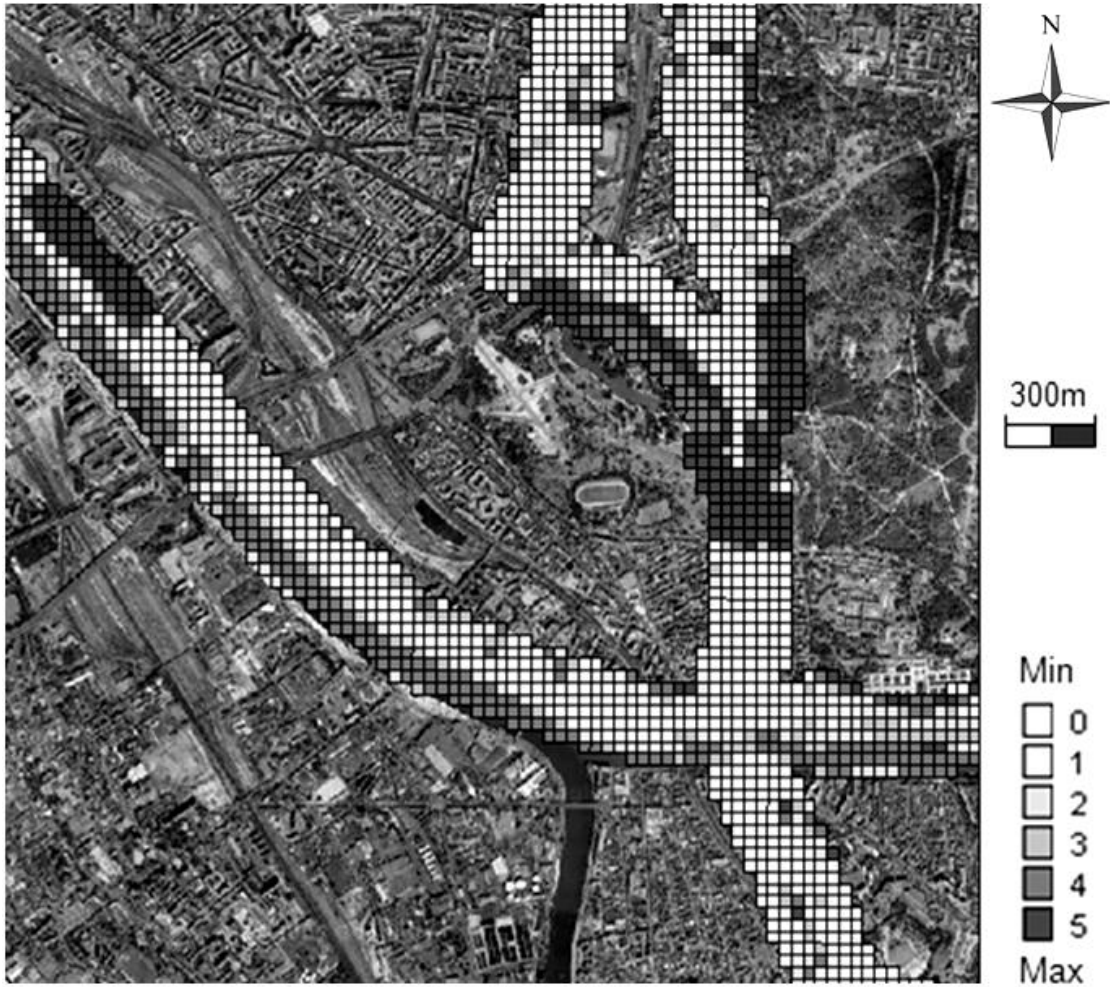


Figure 26: map of environmental risk.

The example shown below (Figure 27) is located south of the “Bois de Vincennes”, along a highway, near the Seine. The human risk around the highway section is calculated (on the bottom right) and CARTENJEUX gives the possibility for the user to consult both the severity index (top right) and the human vulnerability (middle right).

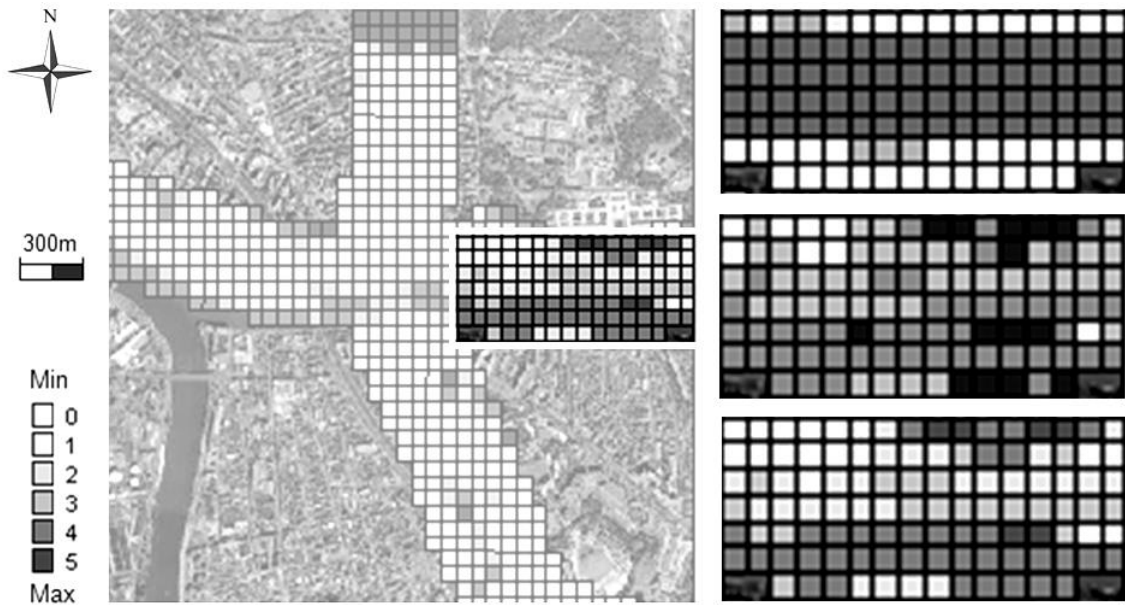


Figure 27: severity index (top right), human vulnerability (middle right) and human risk (bottom right) maps of the same area (south of the Bois de Vincennes).

As we can see, the human vulnerability layer presents some disparities due to urbanized areas which are heterogeneously distributed on either side of the highway. Although the severity index is uniform along the route section, we notice an area (North West on the bottom right map) where the level of human risk is low. Indeed, the human vulnerability is the lowest of this study area at this point due to the presence of a large park (so it is not a very urbanized area). Thus, the same average level of risk can be measured either by combination of a high severity index with a very low vulnerability in one area or by combination of a low severity index with high vulnerability in another.

On the one hand, the weighting of the vulnerability by severity of accident gives an integrated overview of the risk encountered in the case of an accident in this area. On the other hand, it is possible to see that the visual interpretation of results may be a source of errors because the use of color is not a robust way to provide rich information.

That is why, the statistical module of CARTENJEUX (Figure 28), which produces index of vulnerability, severity of accident and risk for human, infrastructural and environmental high-stake elements, is a good additional source of information.

Statistiques			
VULNERABILITY	Minimum	Maximum	Average
Human	0	5	0.959896
Infrastructural	0	5	2.28171
Environmental	0	3	1.18851
SEVERITY	Minimum	Maximum	Average
Human	0	5	2.62783
Infrastructural	0	5	1.9819
Environmental	0	5	1.9819
RISK	Minimum	Maximum	Average
Human	0	25	2.50554
Infrastructural	0	25	4.23394
Environmental	0	15	2.20596

Fermer

Figure 28: statistical summary of the study area.

Figure 29 below shows a former and a new supply strategy. This example aims to study the relocation of a hydrocarbon depot 20km away (new route departure). The arrival point is the same gas station. The initial route is named “#1” and the new one is named “#2”. The delivered quantity of hydrocarbon is the same but there is necessarily a variation in the severity index because the route (and thus the hazard) changes (“#2” follows a new highway). Figure 29 also shows the vulnerability levels of newly assigned high-stake elements, and the impact on the risk levels.

Route #1		→	Route #2a	
<b>Vulnerability [0 to 5]</b>				
Human	0.96	↘ 27%	Human	0.70
Infrastructural	2.28	↗ 35%	Infrastructural	3.07
Environmental	1.18	↗ 24%	Environmental	1.46
<b>Severity index [0 to 5]</b>				

Human	2.62	↘ 16%	Human	2.20
Infrastructural	1.98	↘ 25%	Infrastructural	1.47
Environmental	1.98	↘ 10%	Environmental	1.79
<b>Risk level [0 to 25]</b>				
Human	2.52	↘ 39%	Human	1.54
Infrastructural	4.51	=	Infrastructural	4.51
Environmental	2.33	↗ 12%	Environmental	2.61

Figure 29: comparison of two supply strategies.

The different stakes located along the two routes lead to heterogeneous levels of vulnerability. But, because “#2” is more secure than “#1”, this strategy reduces the risks of a road accident and thus leads to a decrease in the severity index.

We see with this hypothetical case that level of human risk decreases while the risk levels for the environment increases. The weighting factors of the methodology, which integrate the rise in infrastructural vulnerability and the reduction in the severity index for the same stakes, indicate that there is no change in the infrastructural levels of risk.

## 5 CONCLUSIONS

The project consists in the development of a predictive model for determining whether increasing the flow of hydrocarbon transportation (consequence of relocations) significantly increases risk (for people, infrastructure and the environment) and by how much.

The major contribution of this work is to provide a structured proposition for assessing risk levels using severity and vulnerability indexes depending on the location of a DGT accident. A GIS-based tool implements a structured methodology which is proposed to assess the risk levels of supply routes by determining the severity index, the territorial vulnerability and the risk level. The quantification of the vulnerability of the high-stake elements, combined with the severity index of the hydrocarbon transportation gives the associated risk level. In order to implement the proposed methodology, a development scheme is proposed. On this basis, the identified functionalities are implemented by way

of specific routines to build a grid analysis and to run optimized GIS queries. The result is an integrated user friendly tool named CARTENJEUX. Although the methodology was calibrated for studies in “Ile de France” (including Paris), this operational software, based on a geographical information system, might be applied to another territory or further studies. Decision makers can produce three kinds of thematic maps (vulnerability, severity of accident and risk level) for human, infrastructural and environmental stakes. A statistical module gives also another vision of the results in order to manage risks. CARTENJEUX thus helps to determine the most preferable route for hydrocarbon DGT.

Using the developed GIS-tool, French stakeholders were able to consider the issues globally and achieve better management of DGT in the “Ile de France” region.

#### ACKNOWLEDGMENTS

The authors would like to thank the French ministry of industry (DGEMP) for supporting this research.

#### REFERENCES

Ayral P-A., Sauvagnargues-Lesage S., Tena-Chollet F., Thierion V., 2010, “Les Systèmes d’Information Géographique : mise en œuvre”, Les Techniques de l’Ingénieur, 14p, réf. H7416.

BARPI, 2005, “Bilan des accidents technologiques 1992-2004”, Bureau d'Analyse des Risques et Pollutions Industrielles: 19p, in French.

Bubbico R., Di Cave S., Mazzarotta B., 2004, “Risk analysis for road and rail transport of hazardous materials: a GIS approach”, Journal of Loss Prevention in the Process Industries, Vol 17, Issue 6, pages 483-488.

Bubbico R., Maschio G., Mazzarotta B., Milazzo M. F., Parisi E., 2006, “Risk management of road and rail transport of hazardous materials in Sicily”, *Journal of Loss Prevention in the Process Industries*, Volume 19, Issue 1, pages 32-38.

Chen H., Wood M.D., Linstead C., Maltby E., “Uncertainty analysis in a GIS-based multi-criteria analysis tool for river catchment management”, *Environmental Modelling & Software*, Volume 26, Issue 4, April 2011.

Dandrieux A., Heymes F., Tixier J., Lecysin N., Tena-Chollet F., Spinelli R., Slangen P., Hodin A., Munier L., Lapébie E., Le-Gallic C., Dusserre G., “An integrated methodology research to determine consequences of a vessel destruction”, *ESREL 2006, Safety and Reliability for Managing Risk 18-22 September 2006 – Estoril, Portugal*, p.1965-1972.

DCLG (Department for Communities and Local Government), “Multi-criteria analysis: a manual”, London, 2009.

DDT, 2007, “Risque transport de matières dangereuses”, *Direction Départementale des Territoires de la Loire*, in French.

Fabiano B., Currò F., Palazzi E., Pastorino R., 2002, “A framework for risk assessment and decision-making strategies in dangerous good transportation”, *Journal of Hazardous Materials*, Vol 93, Issue 1, 1, pages 1-15.

Marinoni O., Adkins P., Hajkowicz S., “Water planning in a changing climate: Joint application of cost utility analysis and modern portfolio theory”, *Environmental Modelling & Software*, Volume 26, Issue 1, January 2011.

MEDD, 2005, “Arrêté du 29 septembre 2005 relatif à l'évaluation et à la prise en compte de la probabilité d'occurrence, de la cinétique, de l'intensité des effets et de la gravité des conséquences des accidents potentiels dans les études de dangers des installations classées soumises à autorisation”, *legiFrance*.

Milazzo M.F., Lisi R., Maschio G., Antonioni G., Bonvicini S., Spadoni G., 2002, "HazMat transport through Messina town: from risk analysis suggestions for improving territorial safety", *Journal of Loss Prevention in the Process Industries*, Vol 15, Issue 5, pages 347-356.

Milazzo M.F., Lisi R., Maschio G., Antonioni G., Spadoni G., "A study of land transport of dangerous substances in Eastern Sicily", *Journal of Loss Prevention in the Process Industries*, 23(3): 393-403, 2010.

Oggero A., Darbra R.M., Munoz M., Planas E., Casal J., 2006, "A survey of accident occurring during the transport of hazardous substances by road and rail", *Journal of Hazardous Materials*, Vol 133, Issue 1-3, pages 1-7.

Saaty T. L., 1984, "Décider face à la complexité : une approche analytique multicritère d'aide à la décision", collection université – entreprise, entreprise moderne d'édition, Paris.

Tixier J., Dandrieux A., Dusserre G., Bubbico R., Mazzarotta B., Silvetti B., Hubert E., Rodrigues N., Salvi O., 2006, "Environmental vulnerability assessment in the vicinity of an industrial site in the frame of ARAMIS European project", *Journal of Hazardous Materials*, Vol 130, Issue: 3, pages: 251-264.

Tixier J., Dusserre G., Salvi O., et Gaston D., 2002, "Review of 62 risk analysis methodologies of industrial plants", *Journal of Loss prevention in the process industries*, Vol 15, Issue: 4, pages: 291-303.

Tixier J., Dandrieux A., Dusserre G., Bubbico R., Luccone L.G., Mazzarotta B., Carta R., Di Cave S., Silvetti B., Hubert E., Rodrigues N., Salvi O., Gaston D., "Assessment of the environment vulnerability in the surroundings of an industrial site", ESREL 2003, Maastricht 15-18, June 2003.



Tixier J., Tena-Chollet F., Munier L., Lapébie E., Le-Gallic C. & Dusserre G., “Development of a GIS-based approach for the vulnerability assessment of a territory exposed to a potential risk”, European Safety, Reliability & Data Association, 2012.

Verma M., “Railroad transportation of dangerous goods: A conditional exposure approach to minimize transport risk”, Transportation Research Part C: Emerging Technologies, 19(5):790-802, 2011.

Zerger A., Warren G., Hill P., Robertson D., Weidemann A., Lawton K., “Multi-criteria assessment for linking regional conservation planning and farm-scale actions”, Environmental Modelling & Software, Volume 26, Issue 1, January 2011.